Title

Longitudinal Structure—Function Relationship between Macular Vessel Density and Thickness and Central Visual Field in Early Glaucoma

Journal

Ophthalmology Glaucoma, 5(6)

ISSN

2589-4234

Authors

Mohammadzadeh, Vahid
Moghimi, Sasan
Nishida, Takashi
et al.

Publication Date

2022-11-01

DOI

10.1016/j.ogla.2022.06.004

Peer reviewed

HHS Public Access

Author manuscript

Ophthalmol Glaucoma. Author manuscript; available in PMC 2023 October 23.

Published in final edited form as:

Ophthalmol Glaucoma. 2022 ; 5(6): 648–657. doi:10.1016/j.ogla.2022.06.004.

Longitudinal Structure–Function Relationship Between Macular Vessel Density and Thickness and Central Visual Field in Early Glaucoma

Vahid Mohammadzadeh, MD[*,1], **Sasan Moghimi, MD**[*,1], **Takashi Nishida, MD, PhD**[1], **James A. Proudfoot, MSc**[1], **Medi Eslani, MD**[1], **Alireza Kamalipour, MD**[1], **Nevin El-Nimri, OD, PhD**[1], **Eleonora Micheletti, MD**[1], **Linda M. Zangwill, PhD**[1], **Robert N. Weinreb, MD**[1,2]

[1]Hamilton Glaucoma Center, Shiley Eye Institute, Viterbi Family Department of Ophthalmology, University of California, San Diego, La Jolla, CA, United States.

Abstract

Purpose.—Investigate the relationship of longitudinal changes in macular vessel density (VD) (from optical coherence tomography-angiography-OCTA) and ganglion cell complex (GCC) (from OCT) with central visual field (VF) in early glaucoma eyes.

Design.—Observational cohort.

Participants.—95 eyes, 37 preperimetric and 58 early glaucoma (24–2 VF mean deviation (MD) ≥–6 dB), with average follow–up of 3.8 years and 5.3 visits were included.

Methods.—Whole image (wiVD and wiGCC) and parafoveal scans, as well as localized regions of interest (LROI), hemiretinas of whole image and superior, inferior, temporal and nasal sectors of parafoveal maps, were matched with central VF locations. Age-adjusted rates of change of VD, GCC, mean sensitivity (MS) of VF locations and 10–2 VF MD were calculated with linear-mixed–effect models. Normalized rates of change were calculated for comparing between change rates in wiVD and wiGCC.

Main Outcome Measure.—Structure-function (SF) correlations between VD/GCC and central VF measurement change rates and comparison between the correlations of SF relationships after bootstrapping the difference of the correlations.

Results.—VD loss and GCC thinning demonstrated significant correlations with central VF damage, globally and with most LROIs. The SF correlation (r, 95% confidence interval (CI)) was 0.42 (0.24, 0.58) between wiVD and 10–2 VF MD change rates and was 0.27 (0.08, 0.45) between wiGCC and 10–2 VF MD changes rates, all $P < 0.05$. In contrast to GCC thinning, VD loss in the parafoveal sectors demonstrated significant correlations with central VF damage in inferior and temporal sectors. Differences between the SF relationship with central VF damage was not significant between VD loss and GCC thinning. The mean (95% CI) of normalized change rates of wiVD (−7.40 ((−7.71, −7.09)%/year) was faster than wiGCC (−1.95 ((−2.21, −1.70)%/year), $P<0.05$.

[2]**Corresponding author**: Robert N. Weinreb, MD, University of California, San Diego, 9500 Campus Point Drive, La Jolla, CA, 92093-0946, rweinreb@ucsd.edu.

*These authors had equal contributions as co-first authors.

Conclusion.—Rates of VD loss and GCC thinning are associated with central VF loss over time. Assessment of both macular VD and GCC thickness should be considered for evaluation of glaucoma progression.

Precis

Macular vessel density and ganglion cell thickness demonstrated a significant longitudinal structure-function relationship with the central visual field damage over time, in early glaucoma. Evaluation of both should be considered for monitoring of glaucoma progression.

Introduction

Glaucomatous damage is characterized by loss of retinal ganglion cells (RGC) which results in progressive functional loss with loss of visual field (VF).[1,2] Spectral-domain optical coherence tomography (SD–OCT) of the macular is used to assess the central RGC–axonal complex.[3,4] In addition to the damaging effects of intraocular pressure, there is considerable evidence for alterations of vascular blood flow in the pathogenesis of glaucoma.[5–7] Impaired blood flow results in loss of RGCs and thinning of the ganglion cell layer. Optical coherence tomography angiography (OCTA) provides a noninvasive and repeatable evaluation of vasculature in the optic nerve and macula.[8,9]

Evaluation of change of vessel density (VD) with OCTA is a promising approach for the detection of glaucoma progression.[10–13] A strong correlation between VD dropout and the level of glaucoma severity has been shown in several studies.[14–17] However, these studies have evaluated cross-sectional relationships between VD dropout and VF global indices. One study showed a moderate correlation between macular VD dropout and localized central VF locations[18] However, prior studies have not examined the longitudinal structure-function (SF) relationship between macular VD loss and visual field parameters.

A number of studies have documented central VF loss in early glaucoma.[19–25] It has been reported that both macular OCT and central VF are beneficial for detection of glaucomatous defects in early glaucoma.[26] In a recent study by Leung et al., it has been shown that papillofoveal and papillomacular bundles had defects in early glaucoma and the damage was associated with damage in the corresponding VF locations.[27] In their study, only 25.0% of eyes with early glaucoma had arcuate bundle defects without involvement of papillomacular and papillofoveal bundles. Garg et al. reported higher rates of glaucoma progression in eyes that demonstrated central VF damage.[19] In another study, a stronger association between central VF and quality of life was reported in comparison to peripheral VF.[22] The purpose of the current study was to investigate the longitudinal SF relationship between macular VD loss over time and central VF measurements in the early stages of glaucoma.

Methods

Participants

Ninety–five eyes from 70 patients, 37 preperimetric and 58 early primary open angle glaucoma (POAG) patients from the Diagnostic Innovations in Glaucoma Study (DIGS) were enrolled in this study.[28,29] Patients underwent serial OCTA and macular SD–OCT

(Angiovue; Optovue Inc. Fremont, CA, USA) images, and central VF exams[8,9,30–35]. The protocol of the study was approved by institutional review board of University of California, San Diego. Written informed consent was obtained from all participants and the methodology of the study was adherent to Declaration of Helsinki and the Health Insurance Portability and Accountability Act.

Eligible patients were required to have at least two years of follow up with a minimum of 4 OCTA and macular SD–OCT images and central VF exams. Inclusion criteria also included older than 18 years of age, open angles defined by gonioscopy, and a best–corrected visual acuity of 20/40 or better at study entry. Exclusion criteria was history of intraocular surgery (except for uncomplicated glaucoma and cataract surgery), secondary causes of elevated intraocular pressure (IOP), other intraocular eye disease, and axial length of 27 mm or more. Participants with the diagnosis of systemic diseases such as Parkinson's disease, Alzheimer's disease, dementia, or a history of stroke were also excluded.

The criteria for POAG patients, based on 24–2 VF damage, were as follow: glaucoma hemifield test outside normal limit and pattern standard deviation outside less than 5% of normal on at least 2 consecutive exams.[36] The reliability criteria for VF exams were false positive (FP) ≤ 15% and fixation loss (FL) and false negative (FN) ≤ 33%. Early glaucoma was defined as baseline 24–2 mean deviation (MD) ≥ −6. Preperimetric glaucoma included eyes with elevated IOP (≥22mmHg) or glaucomatous-appearing optic discs without the presence of repeatable glaucomatous VF damage. Glaucomatous-appearing optic disc was defined as notching, neuroretinal narrowing, excavation, localized or diffuse retinal nerve fiber layer defect[10,28]

OCTA and SD–OCT imaging

Optical coherence tomography angiography and macular SD–OCT were acquired with AngioVue (Optovue, Inc, Fremont, CA). This imaging system (software version 5.6.3.0) is composed of both angiography and SD–OCT platform and therefore in the same examination, it provides both vascular measurement parameters and thickness of macula between internal limiting membrane (ILM) and inner plexiform layer (IPL), known as GCC.

Macula 3×3–mm^2 scans, centered on fovea and composed of 304 B–scans × 304 A–scans per B–scan, were obtained with AngioVue imaging system. To calculate VD, split–spectrum amplitude– decorrelation angiography (SSADA) method is applied on the scan slab. The AngioVue software is equipped with automatic segmentation and superficial retinal capillary, located between ILM and IPL. The SSADA capture the dynamic motion of the red blood cells and provide a high–resolution 3–dimensional visualization of perfused retinal vasculature. In the next step, VD is calculated as the percentage of area occupied by blood vessels in any specific location. For this study, the VD 3×3–mm^2 whole image (wiVD) and parafoveal VD (pfVD) maps were analyzed. The localized regions of interest (LROI) were the superior and inferior hemiretina of the wiVD, map and the standard instrument defined superior, inferior, temporal and nasal sectors of pfVD map.

The same macular cube provides thickness measurements of GCC. The areas of interest were the 3×3–mm^2 whole image GCC (wiGCC) and parafovea GCC (pfGCC) maps and the

LROI described above, the superior and inferior hemiretina of the wiGCC map and superior, inferior, temporal and nasal sectors of pfGCC map.

The quality of OCTA and SD–OCT images were reviewed according to the protocol of the Imaging Data Evaluation and Analysis Reading Center on all the scans which were processed by the AngioVue software.[37] Trained reviewers evaluated the scans and images and excluded the poor–quality images with the following definitions: 1) scan quality less than 4; 2) poor clarity images; 3) residual motion artifacts visible as an irregular vessel; 4) weak signals in local areas due to media opacity; 5) uncorrectable segmentation errors.

Visual field testing

Central VF was tested with a 10–2 pattern of Humphrey Field Analyzer (Carl Zeiss Meditec®, Dublin, CA). As a matching protocol, VF visits that were within six months of OCTA and SD–OCT visits were selected. The reliability criteria were FL and FN ≤ 33% and FP ≤ 15%. This software measures VF sensitivity at 68 locations in central 10° which are 2° apart vertically and horizontally. The quality of the visual field tests was reviewed by the Visual Field Assessment Center (VisFACT). The VF data were exported as an XML file and 10–2 MD and threshold sensitivity for each location were extracted.

Mapping OCTA VD and SD–OCT GCC maps and 10–2 VF measurements

The 3×3–mm^2 scans approximately cover the central 9° of the macula. The correspondence of structural and functional parameters was based on the central VF locations that occupy a specific area of the scan, after adjusting for RGC displacement, as shown in figure 1.[18,38,39] The VF locations were flipped vertically so that they matched the corresponding anatomic areas in the presented images. A total of 8 central locations corresponded to the wiVD and wiGCC maps (4 VF locations per each hemiretina), while for the parafovea map, 4 central locations were matched, with one location per each sector (Figure 1). To calculate the mean sensitivity (MS) of the cluster of VF locations, the threshold sensitivity of each location was converted to the lambert scale and consequently was averaged into the MS of those locations. The averaged MS value was converted back to a logarithmic scale for further analysis.

Statistical analysis

Demographic characteristics were reported as mean (95% confidence interval (CI)) for continuous variables and count (percentage) for categorical variables. Rates of change of VD, GCC and VF MD and MS/threshold sensitivity at each indicator were investigated with linear mixed effect, with random eye–patients intercept and independent random slopes within eyes. This model provides the ability to obtain the best linear unbiased prediction (BLUP).[40,41] The BLUP accounts for individual measurements and estimates of the linear mixed effect which is applied to the entire sample. This method represents inter-subject heterogeneity by using random slopes and intercepts to introduce subject deviation from the average dataset.[42]

The SF correlation between OCTA and OCT parameters and VF measurement was evaluated with the parametric method. Structure-function correlations will be reported as Pearson's "r" and the corresponding 95% CI and P-value.

To investigate the difference between the SF relationship between VD loss and central VF damage and the SF relationship between GCC thinning and central VF damage, the difference of correlations was performed with bootstrapping 10000 times.[43] This approach provides a normal distribution of the difference between the SF correlations and the average difference along with 95% CI was reported. The difference in the SF correlations was provided for both global indices and the LROI. If zero was included in the 95% CI, the difference between the SF correlations was statistically nonsignificant.

Comparison between rates of change of VD and GCC for this group of POAG eyes at the whole and parafovea images were evaluated using a linear mixed-effect model. For this purpose, since the measures differ in the range of values and units, dynamic range–based normalized coefficients from VD and GCC thickness were estimated.[44] In this method, the means of the lowest and highest 3% (quantiles) of eyes were calculated to define the dynamic range. The percent of dynamic range change, i.e., normalized variable, was then calculated using the following formula: [(visit value –floor value) / dynamic range] × 100. Age-adjusted normalized slopes were measured through the linear mixed effect model described above. Simple linear regression between the normalized slopes of VD and GCC was performed and R^2 value and P value were reported.

Statistical analyses were performed using statistical software R version 4.0.4 (R Foundation for Statistical Computing, Vienna, Austria).[45] P values less than 0.05 were considered statistically significant.

Results

A total of 95 eyes from 70 patients with early-stage glaucoma were included in this study. Table 1 represents the demographic characteristics of the study eyes. The mean (95% confidence interval (CI)) of follow-up time and the number of visits were 3.8 (3.7, 4.0) years and 5.3 (5.0, 5.6) visits, respectively. The average (95% CI) baseline 10° VF MD and 24–2 MD were −1.1(−1.6, −0.7) dB and −1.4(−1.7, −1.0) dB, respectively. Eighty-one eyes (85%) received at least one IOP lowering medication during the follow-up period.

For the global parameters, the mean (95% CI) age-adjusted rates of change of wiVD, wiGCC, pfVD and pfGCC were −1.02 %/year (−1.08, −0.97), −0.93 μm/year (−1.14, −0.72), −0.94 %/year (−1.00, −0.88) and −0.96 μm/year (−1.20, −0.72), respectively (Table 2). The LROIs of the whole image and parafoveal VD map had a range of average change rates between −1.37 %/year (parafoveal temporal sector) and −0.36 %/year (parafoveal nasal sector) and for the GCC parameters, the range of average change rates was between −1.04 μm/year (parafoveal nasal sector) and −0.84 μm/year (parafoveal temporal sector).

Table 3 summarizes the correlation for structural and functional rates of change at global whole image vessel density, parafoveal vessel density and GCC maps and the LROIs. For the whole image vessel density map, the correlation coefficient (r, 95% CI) between wiVD

change rates and 10–2 VF MD change rates was 0.42 (0.24, 0.58), P < 0.001, (Figure 2 A). For the LROIs, the topographic correlation (r, (95% CI)) between wiVD change rates and MS change rate of the central 8 VF locations was 0.26 (0.06, 0.44), P = 0.013, while the SF correlation (r (95% CI)) for superior hemiretina was 0.32 (0.13, 0.49), P = 0.001 and for inferior hemiretina was 0.31 (0.12, 0.48), P = 0.001. The correlation (r (95% CI)) of the pfVD map change rates and MS change rate of the 4 central locations was 0.21 (0.01, 0.39), P = 0.036. The SF relationship of the LROI of the parafoveal map was significantly higher in inferior sector ((r (95% CI)) 0.24 (0.04, 0.42), P = 0.018) compared to superior sector (0.14 (−0.05, 0.34), P = 0.149). There were similar SF correlations (r (95% CI)) for temporal (0.23 (0.03, 0.41), P = 0.022) and nasal (0.23 (0.03, 0.41), P = 0.024) sectors.

The SF correlation (r (95% CI)) between wiGCC and 10–2 VF MD was 0.27 (0.08, 0.45), P = 0.005 (Figure 2 B). The SF correlation (r (95% CI)) between wiGCC thinning and MS change rates of central 8 VF locations was 0.29 (0.1, 0.47), P = 0.004 and between pfGCC thinning and central 4 VF location MS change rates was 0.22 (0.04, 0.41), P = 0.026. Only superior hemiretina of wiGCC map and superior sector pfGCC map represented statistically significant SF correlation (r (95% CI)) between GCC thinning and VF MS change rates (0.43 (0.26, 0.58), P < 0.001 and 0.25 (0.05, 0.43), P = 0.011, respectively).

The correlations with LROIs of the central VF MS and regional VD and GCC maps differed by sector. There were statistically significant SF correlations at inferior and temporal locations for VD maps, which were not observed in the LROI of the GCC maps. Similarly, there was a significant correlation between the GCC superior sector and VF MS, which was not observed in the VF maps. However, there was no statistically significant difference between the SF relationships with central VF damage for VD loss and GCC thinning correlations for the whole image and parafovea maps and the corresponding LROI (all P values > 0.05 using Bootstrapping method). The average (95% CI) differences were represented in Table 3. Figure 3 represents one case of the study sample, that demonstrates progressive VD from 2015 to 2019 and also, progressive central VF defects were seen in the same period of time. However, GCC thickness is showing nearly stable thickness measurements during this follow-up period.

Normalized VD change rates were faster than normalized GCC thinning over time; −7.40 (−7.71, −7.09) %/year and −2.39 (−2.94, −1.84) %/year for wiVD and wiGCC, and −6.63 (−6.96, −6.30) %/year and −2.24 (−2.79, −1.68) %/year for pfVD and pfGCC (all P < 0.001). Figure 2 C shows the weak, but significant correlation (R^2 =0.12, P < 0.001) between normalized VD and GCC change rates at the whole image map. The R^2 between normalized change rates of VD and GCC was 5% for the parafovea maps.

Discussion

In the cohort of eyes with early glaucoma damage at baseline and the average of 3.8 years of follow-up, modest, but significant longitudinal SF correlations were found between 10–2 VF measurements rates of change and both macular VD loss and macular GCC thinning. The highest longitudinal SF correlations were observed between wiVD and 10–2 VF MD. At the LROI of VD maps, there were statistically significant longitudinal SF correlations at inferior

and temporal locations, which were not observed in the LROI of the GCC maps. in, general, faster-normalized change rates also were observed for global VD loss compared to global GCC thinning over time. These results support that OCTA is a promising structural modality for the detection of glaucoma progression as it is associated with central VF loss.

Although some studies have evaluated the longitudinal SF relationship between macular thickness thinning and central VF damage, there is no report regarding the relationship between longitudinal VD loss and central VF damage over time.[24,46] Such a longitudinal study is particularly important as it would more potentially reflect glaucoma progression and more efficiently estimate the structural and functional status of glaucomatous eyes. In the current study, the correlations were higher when more global parameters were investigated. This finding could be explained by reduced variability observed for global structural and functional parameters.[47] The highest longitudinal SF correlation in this study was around 0.4. Prior studies have also shown a similar longitudinal SF relationship between macular OCT and central VF.[24,46] One reason for this fairly low SF relationship is a relatively short follow-up time in the current study (mean follow-up time of 3.8 years). Moreover, since most of the eyes were receiving treatment during the follow-up period (86%), the magnitude of structural and functional change was relatively small. Finally, RGC damage might cause functional deteriorations that could be detected by functional tests with otherwise normal structural tests.[48,49]

Preserving central VF for glaucoma eyes is an important task for clinicians, especially in the early stages before the eyes reach advanced stages. Compared with the standard 24–2 VF, the central VF involvement more strongly influences the quality of life of glaucoma patients and is an important predictor of glaucoma progression.[22,19] Several studies of SF relationships have focused on the correlation between different structural modalities and the central VF.[24,46,47,50–55] In the current longitudinal study, macular OCTA VD loss and GCC thinning were both associated with central VF change. The significant correlations observed between central VF change rates and both VD and GCC change rates, globally and in most LROI, supports this finding. For SF correlation with 10–2 VF MD, VD loss was stronger than the correlation with GCC thinning, but the difference did not reach statistical significance. This is in agreement with previous cross-sectional studies that reported stronger correlations of VF measurements with VD loss compared with GCC thinning.[14,34,56,57] In the current longitudinal study, faster normalized VD loss in comparison to GCC thinning for these early glaucoma eyes was observed, which was consistent with the previous reports.[10] Therefore, evaluation of VD loss could potentially estimate the overall central functional status of early-stage glaucoma eyes. However, due to the fact that faster rates of VD loss were not always associated with faster rates of central VF change (Figure 2 A), performing both OCTA and central VF would be potentially useful for monitoring glaucoma progression. Further studies are required to be designed to support this finding.

An important strength of our study is the evaluation of the SF relationship longitudinally in LROI of VD and GCC maps. Since glaucoma damage starts locally, it is important to evaluate structural and functional changes in localized areas, especially for early-stage glaucoma eyes. To address the variability of threshold sensitivity of a few central VF

locations, the measurements were averaged to mean sensitivities for wiVD, pfVD and hemiretinas.[48] However, for the parafovea sectors, only one VF location was matched with the anatomical region. Another approach that was used to address the variability was performing BLUP to estimate population slope by applying random slope and random intercept effects. For the parafovea sectors, the VD loss demonstrated significant SF correlations with central VF damage observed at inferior and temporal locations, which was not observed for GCC thinning, where GCC thinning was significantly associated with central VF damage in the superior sector while VD was not. It is unclear why the sectoral associations between VF MD and VD and GCC defer. It has been reported by Hood et al. that glaucoma damage starts at an inferior–temporal location, an area known as the macular vulnerability zone.[53,55,58] The current study showed that OCTA VD loss follows the same structural trend. Regarding the hemiretinas of the whole image maps, VD loss demonstrated significant correlations with central VF damage for both superior and inferior hemiretinas. However, GCC thinning represented a significant correlation with central VF damage only in superior hemiretina. This is in contrast with a previous longitudinal SF study for macular thickness thinning and central VF which demonstrated stronger correlations in inferior hemiretina in advanced glaucoma eyes.[24] To evaluate glaucoma progression in inferior hemiretina for early-stage glaucoma eyes, changes in microvasculature could potentially provide additional structural information.

In this study, no statistically significant difference was found in the SF relationships between both VD loss and GCC thinning with central VF damage. This finding suggests that information from both microvasculature dropout and thickness measurements in the macula can be potentially important in monitoring glaucoma. However, a higher magnitude of SF correlations was observed between VD loss and 10–2 VF MD. Although VD had a higher correlation with central VF, the difference in the correlation of macular OCT with the central VF was not statistically significant. Future studies with larger sample sizes in different stages of glaucoma are needed to better elucidate the SF relationship of OCTA and OCT with central VF. This finding is in agreement with reports from previous studies.[16,59,60] One explanation for this finding is the theory of RGC dysfunction happens before RGC death.[49,61–65] Impaired microvasculature in the macula could result in metabolic stress insufficiency.[6,66] Therefore, VD loss could provide additional structural information which can be used to detect glaucoma progression early in the course of the disease. Additionally, it has been reported that restoration of blood supply and removing the effect of ischemia from the RGCs, could potentially reverse this RGC dysfunction and avoid RGC death.[67]Thus, detection of these early defects may be important for initiating appropriate treatment to stabilize the course of glaucomatous damage.

There are several limitations to this study. First, OCTA scans with poor quality and artifacts have been excluded from the analysis. It has been shown that there is a significant number (approximately 30%) of OCTA images with artifacts.[68,69] Therefore, this analysis represents the correlations using only good-quality images. The variability introduced to the clinical dataset by these artifacts might have an effect on the SF correlation between OCTA and central VF in the actual clinical setting. Second, the incorporation of a larger 6×6 mm^2 could provide a more precise evaluation of SF relationships with central VF.[70] Although not shown in this study, 6×6 mm^2 matched with almost all the 68 locations of central VF. Future

studies with an additional follow-up time of both 6×6 mm^2 maps and central VF could address this limitation. For the third limitation, the effect of different topical and systemic medications on the SF relationship was not considered in this study. However, some reports emphasized the effect of certain medications on vessel density loss.[71,72] Finally, for the parafovea sectors, since there was only one corresponding VF location, the variability of the VF threshold sensitivity could not be diluted by averaging the threshold sensitivities (similar to other LROIs). However, by performing BLUP for calculating the rates of change of VF measurement for those sectors, the intrinsic variability could somehow be reduced.

In conclusion, the SF correlations of VD loss and GCC thinning with central VF change rates were significant in global maps and most of the LROI. Although the correlation of VD loss over time and the rate of central function change were higher than the correlation of GCC thinning over time with central function change in this cohort of early glaucoma eyes, the magnitude of the correlations was only modest. Rates of VD loss and GCC thinning were both associated with central VF loss over time, and assessment of both should be considered for monitoring of the disease and evaluation of glaucoma progression.

Support:

National Eye Institute EY029058, EY11008, EY19869, EY14267, EY027510, EY026574, P30EY022589, and participant retention incentive grants in the form of glaucoma medication at no cost from Novartis/Alcon Laboratories Inc, Allergan, Akorn, and Pfizer Inc. Unrestricted grant from Research to Prevent Blindness, New York, New York

References

1. Weinreb RN, Aung T, Medeiros FA. The pathophysiology and treatment of glaucoma: a review. JAMA. 2014;311(18):1901–1911. [PubMed: 24825645]
2. Weinreb RN, Khaw PT. Primary open-angle glaucoma. Lancet. 2004;363(9422):1711–1720. [PubMed: 15158634]
3. Mohammadzadeh V, Fatehi N, Yarmohammadi A, et al. Macular imaging with optical coherence tomography in glaucoma. Surv Ophthalmol. 2020;65(6):597–638. [PubMed: 32199939]
4. Wu Z, Weng DSD, Thenappan A, Ritch R, Hood DC. Evaluation of a Region-of-Interest Approach for Detecting Progressive Glaucomatous Macular Damage on Optical Coherence Tomography. Transl Vis Sci Technol. 2018;7(2):14.
5. Weinreb RN. Ocular blood flow in glaucoma. Can J Ophthalmol. 2008;43(3):281–283. [PubMed: 18504463]
6. Flammer JOS, Costa VP, Orzalesi N, Krieglstein GK, Serra LM, Renard JP, Stefánsson E. The impact of ocular blood flow in glaucoma. . Prog Retin Eye Res. 2002 Jul 1;21(4):359–393. [PubMed: 12150988]
7. Chan KKW, Tang F, Tham CCY, Young AL, Cheung CY. Retinal vasculature in glaucoma: a review. BMJ Open Ophthalmol. 2017;1(1):e000032.
8. Moghimi S, Hou H, Rao H, Weinreb RN. Optical Coherence Tomography Angiography and Glaucoma: A Brief Review. Asia Pac J Ophthalmol (Phila). 2019.
9. Rao HL, Pradhan ZS, Suh MH, Moghimi S, Mansouri K, Weinreb RN. Optical Coherence Tomography Angiography in Glaucoma. J Glaucoma. 2020;29(4):312–321. [PubMed: 32053551]
10. Hou H, Moghimi S, Proudfoot JA, et al. Ganglion Cell Complex Thickness and Macular Vessel Density Loss in Primary Open-Angle Glaucoma. Ophthalmology. 2020;127(8):1043–1052. [PubMed: 32085875]

11. Shoji T, Zangwill LM, Akagi T, et al. Progressive Macula Vessel Density Loss in Primary Open-Angle Glaucoma: A Longitudinal Study. Am J Ophthalmol. 2017;182:107–117. [PubMed: 28734815]
12. Manalastas PIC, Zangwill LM, Saunders LJ, et al. Reproducibility of Optical Coherence Tomography Angiography Macular and Optic Nerve Head Vascular Density in Glaucoma and Healthy Eyes. J Glaucoma. 2017;26(10):851–859. [PubMed: 28858159]
13. Venugopal JP, Rao HL, Weinreb RN, et al. Repeatability of vessel density measurements of optical coherence tomography angiography in normal and glaucoma eyes. Br J Ophthalmol. 2018;102(3):352–357. [PubMed: 28739645]
14. Yarmohammadi A, Zangwill LM, Diniz-Filho A, et al. Relationship between Optical Coherence Tomography Angiography Vessel Density and Severity of Visual Field Loss in Glaucoma. Ophthalmology. 2016;123(12):2498–2508. [PubMed: 27726964]
15. Ghahari E, Bowd C, Zangwill LM, et al. Association of Macular and Circumpapillary Microvasculature with Visual Field Sensitivity in Advanced Glaucoma. Am J Ophthalmol. 2019;204:51–61. [PubMed: 30878489]
16. Yarmohammadi A, Zangwill LM, Diniz-Filho A, et al. Peripapillary and Macular Vessel Density in Patients with Glaucoma and Single-Hemifield Visual Field Defect. Ophthalmology. 2017;124(5):709–719. [PubMed: 28196732]
17. Yarmohammadi A, Zangwill LM, Manalastas PIC, et al. Peripapillary and Macular Vessel Density in Patients with Primary Open-Angle Glaucoma and Unilateral Visual Field Loss. Ophthalmology. 2018;125(4):578–587. [PubMed: 29174012]
18. Penteado RC, Zangwill LM, Daga FB, et al. Optical Coherence Tomography Angiography Macular Vascular Density Measurements and the Central 10–2 Visual Field in Glaucoma. J Glaucoma. 2018;27(6):481–489. [PubMed: 29664832]
19. Garg A, De Moraes CG, Cioffi GA, et al. Baseline 24–2 Central Visual Field Damage Is Predictive of Global Progressive Field Loss. Am J Ophthalmol. 2018;187:92–98. [PubMed: 29317211]
20. Odden JL, Mihailovic A, Boland MV, Friedman DS, West SK, Ramulu PY. Evaluation of Central and Peripheral Visual Field Concordance in Glaucoma. Invest Ophthalmol Vis Sci. 2016;57(6):2797–2804. [PubMed: 27214688]
21. Weiner A, Ripkin DJ, Patel S, Kaufman SR, Kohn HD, Weidenthal DT. Foveal dysfunction and central visual field loss in glaucoma. Arch Ophthalmol. 1998;116(9):1169–1174. [PubMed: 9747674]
22. Blumberg DM, De Moraes CG, Prager AJ, et al. Association Between Undetected 10–2 Visual Field Damage and Vision-Related Quality of Life in Patients With Glaucoma. JAMA Ophthalmol. 2017;135(7):742–747. [PubMed: 28542692]
23. Roberti G, Manni G, Riva I, et al. Detection of central visual field defects in early glaucomatous eyes: Comparison of Humphrey and Octopus perimetry. PLoS One. 2017;12(10):e0186793. [PubMed: 29077730]
24. Mohammadzadeh V, Rabiolo A, Fu Q, et al. Longitudinal Macular Structure-Function Relationships in Glaucoma. Ophthalmology. 2020 Jul 1;127(7):888–900. [PubMed: 32173112]
25. Tatham AJ, Weinreb RN, Medeiros FA. Strategies for improving early detection of glaucoma: the combined structure-function index. Clin Ophthalmol. 2014;8:611–621. [PubMed: 24707166]
26. Hood DC, Slobodnick A, Raza AS, de Moraes CG, Teng CC, Ritch R. Early glaucoma involves both deep local, and shallow widespread, retinal nerve fiber damage of the macular region. Invest Ophthalmol Vis Sci. 2014;55(2):632–649. [PubMed: 24370831]
27. Leung CKS, Guo PY, Lam AKN. Retinal Nerve Fiber Layer Optical Texture Analysis (ROTA): Involvement of the Papillomacular Bundle and Papillofoveal Bundle in Early Glaucoma. Ophthalmology. 2022.
28. Sample PA, Girkin CA, Zangwill LM, et al. The African Descent and Glaucoma Evaluation Study (ADAGES): design and baseline data. Arch Ophthalmol. 2009;127(9):1136–1145. [PubMed: 19752422]
29. Girkin CA, Sample PA, Liebmann JM, et al. African Descent and Glaucoma Evaluation Study (ADAGES): II. Ancestry differences in optic disc, retinal nerve fiber layer, and macular structure in healthy subjects. Arch Ophthalmol. 2010;128(5):541–550. [PubMed: 20457974]

30. Spaide RF, Fujimoto JG, Waheed NK, Sadda SR, Staurenghi G. Optical coherence tomography angiography. Prog Retin Eye Res. 2018;64:1–55. [PubMed: 29229445]
31. Yarmohammadi A, Zangwill LM, Diniz-Filho A, et al. Optical Coherence Tomography Angiography Vessel Density in Healthy, Glaucoma Suspect, and Glaucoma Eyes. Invest Ophthalmol Vis Sci. 2016;57(9):OCT451–459. [PubMed: 27409505]
32. Yu J, Jiang C, Wang X, et al. Macular perfusion in healthy Chinese: an optical coherence tomography angiogram study. Invest Ophthalmol Vis Sci. 2015;56(5):3212–3217. [PubMed: 26024105]
33. Liu L, Jia Y, Takusagawa HL, et al. Optical Coherence Tomography Angiography of the Peripapillary Retina in Glaucoma. JAMA Ophthalmol. 2015;133(9):1045–1052. [PubMed: 26203793]
34. Jia Y, Wei E, Wang X, et al. Optical coherence tomography angiography of optic disc perfusion in glaucoma. Ophthalmology. 2014;121(7):1322–1332. [PubMed: 24629312]
35. Rao HL, Srinivasan T, Pradhan ZS, et al. Optical Coherence Tomography Angiography and Visual Field Progression in Primary Angle Closure Glaucoma. J Glaucoma. 2021;30(3):e61–e67. [PubMed: 33273281]
36. Hodapp E, Parrish II RK, Anderson DR. Clinical decisions in glaucoma. First ed. St. Louis: Mosby; 1993.
37. Hou H, Moghimi S, Zangwill LM, et al. Macula Vessel Density and Thickness in Early Primary Open-Angle Glaucoma. Am J Ophthalmol. 2019;199:120–132. [PubMed: 30496723]
38. Drasdo N, Millican CL, Katholi CR, Curcio CA. The length of Henle fibers in the human retina and a model of ganglion receptive field density in the visual field. Vision Res. 2007;47(22):2901–2911. [PubMed: 17320143]
39. Raza AS, Cho J, de Moraes CG, et al. Retinal ganglion cell layer thickness and local visual field sensitivity in glaucoma. Arch Ophthalmol. 2011;129(12):1529–1536. [PubMed: 22159673]
40. Laird NM, Donnelly C, Ware JH. Longitudinal studies with continuous responses. Stat Methods Med Res. 1992;1(3):225–247. [PubMed: 1341659]
41. Laird NM, Ware JH. Random-Effects Models for Longitudinal Data. Biometrics. 1982;38(4).
42. Robinson GK. That BLUP is a good thing: the estimation of random effects. Statistical science. 1991 Feb 1:15–32.
43. Deng NAJ, Fang HJ. Using the bootstrap to establish statistical significance for relative validity comparisons among patient-reported outcome measures. Health and Quality of Life Outcomes. 2013:11:89. [PubMed: 23721463]
44. Hammel N, Belghith A, Weinreb RN, Medeiros FA, Mendoza N, Zangwill LM. Comparing the Rates of Retinal Nerve Fiber Layer and Ganglion Cell-Inner Plexiform Layer Loss in Healthy Eyes and in Glaucoma Eyes. Am J Ophthalmol. 2017;178:38–50. [PubMed: 28315655]
45. RC TR: A language and environment for statistical computing. R Foundation for Statistical Computing, Vienna, Austria 2013.
46. Suda K, Hangai M, Akagi T, et al. Comparison of Longitudinal Changes in Functional and Structural Measures for Evaluating Progression of Glaucomatous Optic Neuropathy. Invest Ophthalmol Vis Sci. 2015;56(9):5477–5484. [PubMed: 26284553]
47. Nouri-Mahdavi K, Fatehi N, Caprioli J. Longitudinal Macular Structure-Function Relationships in Glaucoma and Their Sources of Variability. Am J Ophthalmol. 2019;207:18–36. [PubMed: 31078529]
48. Denniss J, Turpin A, McKendrick AM. Relating optical coherence tomography to visual fields in glaucoma: structure-function mapping, limitations and future applications. Clin Exp Optom. 2018.
49. Fry LE, Fahy E, Chrysostomou V, et al. The coma in glaucoma: Retinal ganglion cell dysfunction and recovery. Prog Retin Eye Res. 2018;65:77–92. [PubMed: 29631042]
50. Rao HL, Qasim M, Hussain RS, et al. Structure-Function Relationship in Glaucoma Using Ganglion Cell-Inner Plexiform Layer Thickness Measurements. Invest Ophthalmol Vis Sci. 2015;56(6):3883–3888. [PubMed: 26070060]
51. Raza AS, Cho J, de Moraes CG, et al. Retinal ganglion cell layer thickness and local visual field sensitivity in glaucoma. Arch Ophthalmol. 2011;129(12):1529–1536. [PubMed: 22159673]

52. Hood DC, Raza AS, de Moraes CG, Johnson CA, Liebmann JM, Ritch R. The Nature of Macular Damage in Glaucoma as Revealed by Averaging Optical Coherence Tomography Data. Transl Vis Sci Technol. 2012;1(1):3.
53. Hood DC. Improving our understanding, and detection, of glaucomatous damage: An approach based upon optical coherence tomography (OCT). Prog Retin Eye Res. 2017;57:46–75. [PubMed: 28012881]
54. Hood DC, Kardon RH. A framework for comparing structural and functional measures of glaucomatous damage. Prog Retin Eye Res. 2007;26(6):688–710. [PubMed: 17889587]
55. Hood DC, Raza AS, de Moraes CG, Liebmann JM, Ritch R. Glaucomatous damage of the macula. Prog Retin Eye Res. 2013;32:1–21. [PubMed: 22995953]
56. Shin JW, Lee J, Kwon J, Choi J, Kook MS. Regional vascular density-visual field sensitivity relationship in glaucoma according to disease severity. Br J Ophthalmol. 2017;101(12):1666–1672. [PubMed: 28432111]
57. Chen HS, Liu CH, Wu WC, Tseng HJ, Lee YS. Optical Coherence Tomography Angiography of the Superficial Microvasculature in the Macular and Peripapillary Areas in Glaucomatous and Healthy Eyes. Invest Ophthalmol Vis Sci. 2017;58(9):3637–3645. [PubMed: 28728171]
58. Hood DC RA. Method for comparing visual field defects to local RNFL and RGC damage seen on frequency domain OCT in patients with glaucoma. Biomedical optics express. 2011 May 1;2(5):1097–1105. [PubMed: 21559122]
59. Chen CL, Bojikian KD, Wen JC, et al. Peripapillary Retinal Nerve Fiber Layer Vascular Microcirculation in Eyes With Glaucoma and Single-Hemifield Visual Field Loss. JAMA Ophthalmol. 2017;135(5):461–468. [PubMed: 28358939]
60. Pradhan ZS DS, Sreenivasaiah S, Rao HL, Venugopal JP, Devi S, Webers CA. . A sectoral analysis of vessel density measurements in perimetrically intact regions of glaucomatous eyes: an optical coherence tomography angiography study. ;27(6):525–31. Journal of glaucoma 2018 Jun 1;27(6):525–531. [PubMed: 29557826]
61. Porciatti V, Ventura LM. Retinal ganglion cell functional plasticity and optic neuropathy: a comprehensive model. J Neuroophthalmol. 2012;32(4):354–358. [PubMed: 23196946]
62. Zhao D, Wong VHY, Nguyen CTO, et al. Reversibility of Retinal Ganglion Cell Dysfunction From Chronic IOP Elevation. Invest Ophthalmol Vis Sci. 2019;60(12):3878–3886. [PubMed: 31529082]
63. VanderWall KB, Lu B, Alfaro JS, et al. Differential susceptibility of retinal ganglion cell subtypes in acute and chronic models of injury and disease. Sci Rep. 2020;10(1):17359. [PubMed: 33060618]
64. Gasser PFJ. Blood-cell velocity in the nailfold capillaries of patients with normal-tension and high-tension glaucoma. Am J Ophthalmol. 1991 May 1;111(5):585–588. [PubMed: 2021167]
65. Nicolela MT WB, Buckley AR, Drance SM. Ocular hypertension and primary open-angle glaucoma: a comparative study of their retrobulbar blood flow velocity. J Glaucoma. 1996 Oct 1;5(5):308–310. [PubMed: 8897229]
66. Leske MC. Ocular perfusion pressure and glaucoma: clinical trial and epidemiologic findings. Curr Opin Ophthalmol. 2009;20(2):73–78. [PubMed: 19240538]
67. Siliprandi RBM, Canella R, Carmignoto G. Flash and pattern electroretinograms during and after acute intraocular pressure elevation in cats. Invest Ophthalmol Vis Sci. 1988 Apr 1;29(4):558–565. [PubMed: 3356513]
68. Suh MH, Zangwill LM, Manalastas PI, et al. Optical Coherence Tomography Angiography Vessel Density in Glaucomatous Eyes with Focal Lamina Cribrosa Defects. Ophthalmology. 2016;123(11):2309–2317. [PubMed: 27592175]
69. Kamalipour A, Moghimi S, Hou H, et al. OCT Angiography Artifacts in Glaucoma. Ophthalmology. 2021.
70. Takusagawa HL, Liu L, Ma KN, et al. Projection-Resolved Optical Coherence Tomography Angiography of Macular Retinal Circulation in Glaucoma. Ophthalmology. 2017;124(11):1589–1599. [PubMed: 28676279]
71. Mayama C, Araie M. Effects of antiglaucoma drugs on blood flow of optic nerve heads and related structures. Jpn J Ophthalmol. 2013;57(2):133–149. [PubMed: 23321913]

72. Chihara E, Dimitrova G, Chihara T. Increase in the OCT angiographic peripapillary vessel density by ROCK inhibitor ripasudil instillation: a comparison with brimonidine. Graefes Arch Clin Exp Ophthalmol. 2018;256(7):1257–1264. [PubMed: 29520478]

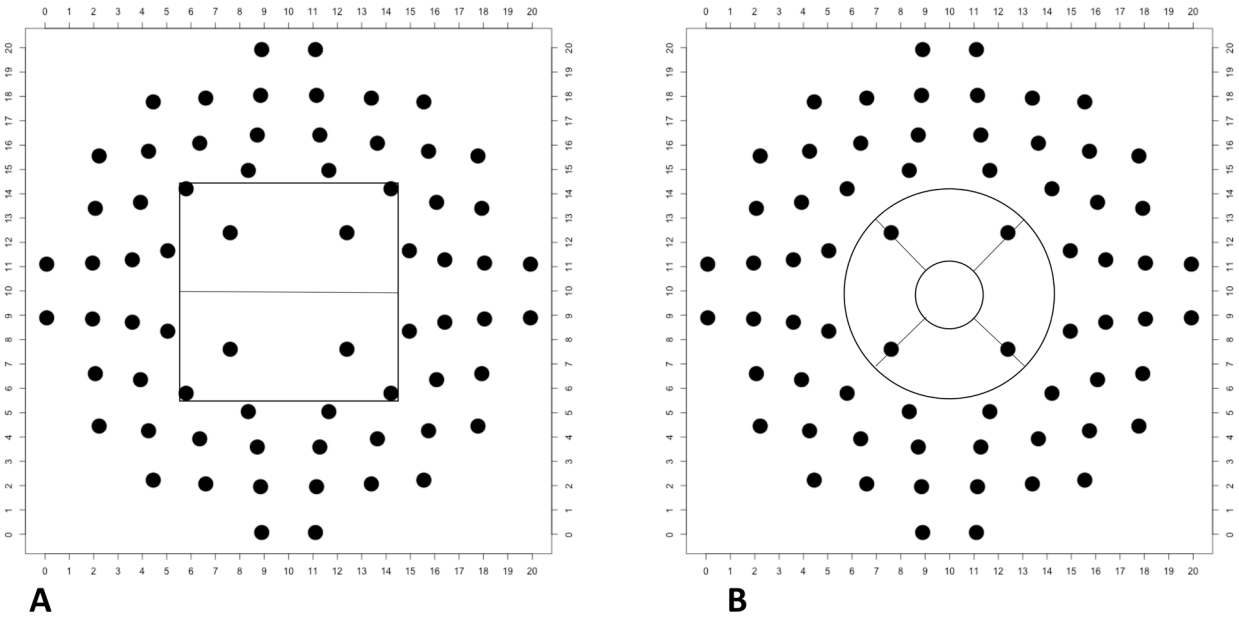

Figure 1.

Mapping 3×3–mm^2 whole image vessel density (VD) and ganglion cell complex (GCC) (A) and parafoveal VD and GCC map with central visual field locations, after adjustment for the displacement of retinal ganglion cells.

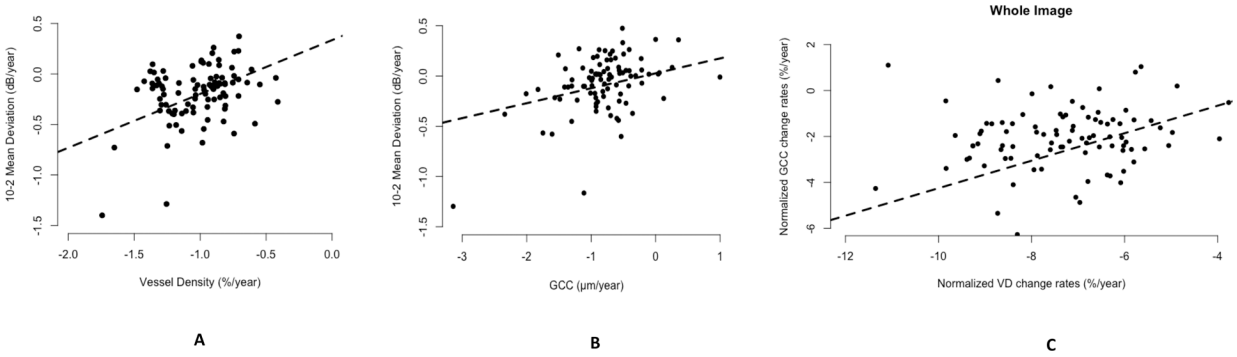

Figure 2.

A) Scatterplot representing structure–function relationship between whole image vessel density and 10–2 visual field mean deviation change rates (r= 0.42 (0.24, 0.58), P < 0.001). **B)** Scatter plot representing structure–function relationship between whole image ganglion cell complex thickness change and 10–2 visual field mean deviation change rates (r= 0.27 (0.08, 0.45), P = 0.005). **C)** Scatter plot representing the correlation between normalized dynamic range–based slopes of vessel density loss and ganglion cell complex thinning at parafovea scan slab (R^2 =0.12, P < 0.001). VD = vessel density; GCC= ganglion cell complex

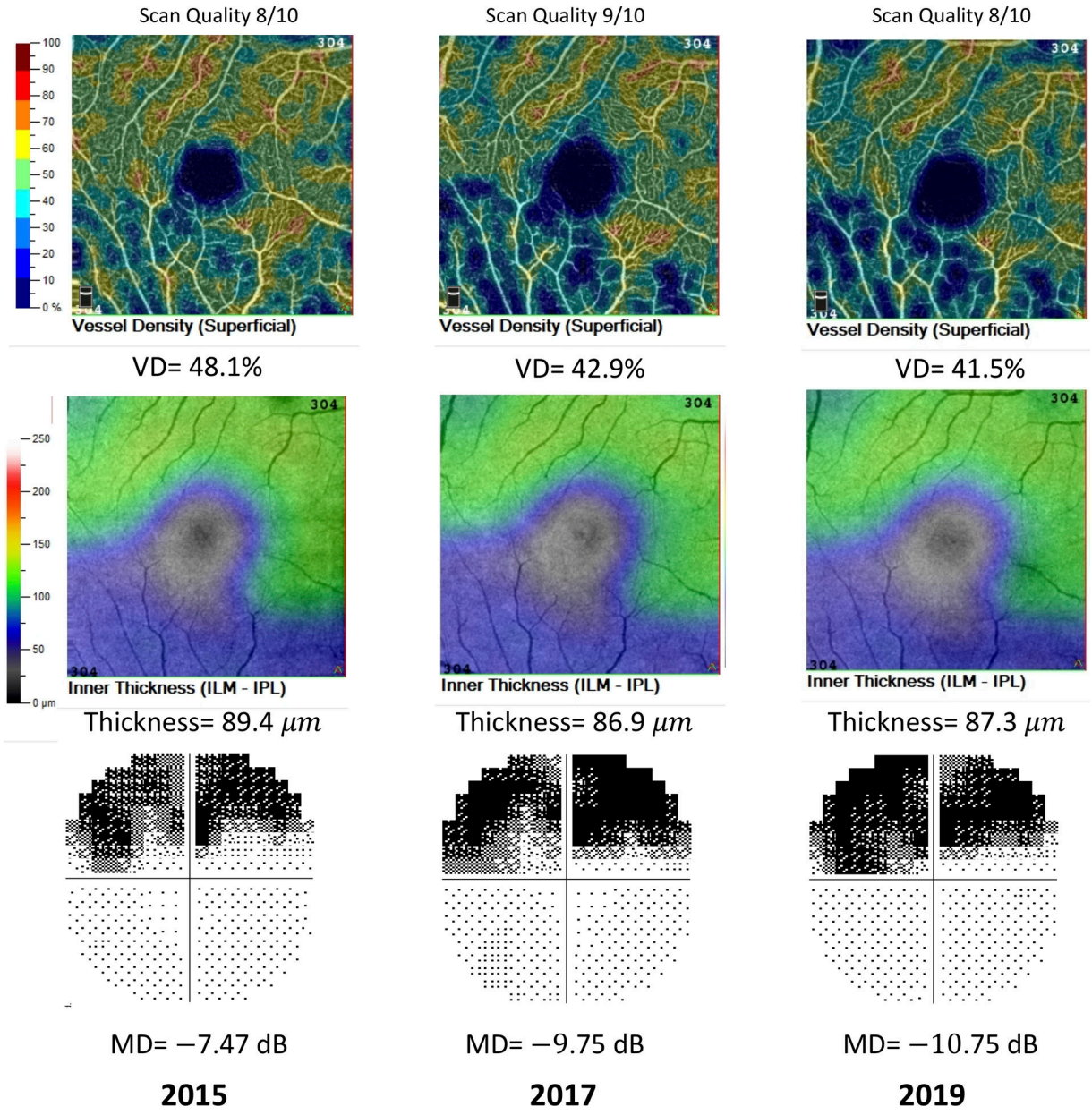

Figure 3.

A representing case followed up from the years 2015 to 2019, demonstrated progressive vessel density (VD) loss (top row), nearly stable ganglion cell complex (GCC) thickness (middle row) and progressive central visual field defect (bottom row).

Table1.

Baseline demographic characteristics of study eyes.

Characteristics	N=70, Eyes=95
Age (years)	68.3 (68.1, 68.6)
Gender (%)	
Female / Male	57 (60%) /38 (40%)
Race (%)	
African American/ Non-African American	28 (30%) / 67 (70%)
Baseline IOP (mmHg)	15.7 (15.6, 15.8)
Baseline CCT (μm)	539.0 (538.1, 539.9)
Diagnosis (%)	
POAG / Glaucoma suspect	58(61%)/37(39%)
Follow up time (years)	3.8 (3.7, 4.0)
Number of exams	5.3 (5.0, 5.6)
Baseline 24–2 MD (dB)	−1.4 (−1.7, −1.0)
Baseline 10–2 MD (dB)	−1.1 (−1.6, −0.7)
Baseline wiVD (%)	45.7 (44.8, 46.5)
Baseline wiGCC (μm)	92.0 (89.8, 94.2)
10–2 MD rates of change (dB/y)	−0.21 (−0.2, −0.1)
wiVD rates of change (%/y)	−1.0 (−1.1, −1.0)
wiGCC rates of change (μm/y)	0.8 (−0.8, −0.7)

IOP = intraocular pressure; CCT = central corneal thickness; POAG = primary open angle glaucoma; MD = mean deviation; wiVD = whole image vessel density; wiGCC = whole image ganglion cell complex. Values are shown in mean (95% confidence interval), unless otherwise indicated.

Table 2.

Age adjusted rates of change of vessel density (VD), ganglion cell complex (GCC) and central visual field mean sensitivity estimated through linear mixed effect model. The mean and 95% confidence interval (CI) are represented for global and sectoral indicators of VD and GCC maps. (N=70 patients, 95 eyes)

	Vessel Density rates (%/year)	Central Visual Field (dB/year)	Ganglion Cell Complex (μm/year)
	Mean (95% CI)	Mean (95% CI)	Mean (95% CI)
Whole Image map	−1.02 (−1.08, −0.97)	−0.14 (−0.18, −0.09)	−0.93 (−1.14, −0.72)
Superior Hemiretina	−0.76 (−0.82, −0.70)	−0.04 (−0.09, 0.02)	−0.96 (−1.19, −0.73)
Inferior Hemiretina	−1.36 (−1.42, −1.31)	−0.32 (−0.39, −0.26)	−0.92 (−1.11, −0.72)
Parafovea map	−0.94 (−1.00, −0.88)	−0.23 (−0.27, −0.18)	−0.96(−1.20, −0.72)
Superior Sector	−0.90 (−0.97, −0.83)	−0.03 (−0.08, 0.02)	−1.00 (−1.26, −0.73)
Inferior Sector	−1.14 (−1.22, −1.06)	−0.77 (−0.84, −0.69)	−0.96 (−1.21, −0.72)
Temporal Sector	−1.37 (−1.44, −1.30)	−0.05 (−0.13, 0.03)	−0.84 (−1.07, −0.62)
Nasal Sector	−0.36 (−0.42, −0.31)	−0.02 (−0.12, 0.07)	−1.04 (−1.27, −0.80)

CI= 95% confidence interval.

Table 3.

Structure-function (SF) correlations (r) between central visual field (VF) defect and age-adjusted vessel density loss and ganglion cell complex thinning. Differences (95% CI) between the two SF relationships are calculated with Bootstrapping methods. The differences between the corresponding SF relationships were considered not significant when the 95% CI contains zero. (N=70 patients, 95 eyes)

	Vessel Density Loss		GCC Thinning		Difference in r (95%CI)
	r Coefficient (95% CI)	P value	r Coefficient (95% CI)	P value	
Whole image and 10–2 MD	0.42 (0.24, 0.58)	< 0.001	0.27 (0.08, 0.45)	0.005	0.14 (−0.29, 0.59)
Whole image and VF MS	0.29 (0.09, 0.46)	0.004	0.29 (0.10, 0.47)	0.004	0.00 (−0.30, 0.29)
Superior Hemiretina	0.32 (0.13, 0.49)	0.001	0.43 (0.26, 0.58)	<0.001	−0.11 (−0.49, 0.17)
Inferior Hemiretina	0.31 (0.12, 0.48)	0.001	0.08 (−0.11, 0.28)	0.410	0.23 (−0.17, 0.71)
Parafovea and VF MS	0.21 (0.01, 0.39)	0.036	0.22 (0.02, 0.41)	0.026	−0.01 (−0.34, 0.28)
Superior Sector	0.14 (−0.05, 0.34)	0.149	0.25 (0.05, 0.43)	0.011	0.10 (−0.40, 0.15)
Inferior Sector	0.24 (0.04, 0.42)	0.018	0.10 (−0.1, 0.3)	0.323	0.13 (−0.23, 0.56)
Temporal Sector	0.23 (0.03, 0.41)	0.022	−0.03 (−0.23, 0.17)	0.771	0.26 (−0.17, 0.79)
Nasal Sector	0.23 (0.03, 0.41)	0.024	0.23 (0.03, 0.41)	0.025	0.00 (−0.51, 0.43)

MD = mean deviation, VF = visual field, MS = mean sensitivity, CI = 95% confidence interval.